

# Covalently bonded assembly and photoluminescent properties of rare earth/silica/poly (methyl methacrylate-co-maleic anhydride) hybrid materials

Bing Yan\*, Qianming Wang

Department of Chemistry, Tongji University, Shanghai 200092, China

Received 3 November 2007; received in revised form 13 December 2007; accepted 26 December 2007

Available online 5 January 2008

## Abstract

Copolymer (MMA-co-MAL) of methyl methacrylate (MMA) and maleic anhydride (MAL) was prepared and grafted by 3-aminopropyltriethoxysilane (APES), which behaves as the structural precursor for functional bridge to assemble the covalently bonded systems through the coordination to rare earth ions ( $\text{Eu}^{3+}$ ,  $\text{Tb}^{3+}$ ) with carboxylic groups of maleic anhydride. On the other hand, 1,10-phenanthroline (phen) is engaged in a second functional ligand to sensitize the luminescence of  $\text{RE}^{3+}$  (rare earth ions) by intramolecular energy transfer process. Meanwhile, the cohydrolysis and copolycondensation processes happened between triethoxysilyl of modified copolymer (MMA-co-MAL-APES) and tetraethoxysilane (TEOS) with Si–O covalent bonds, resulting in the polymer-inorganic hybrids (phen-RE-MMA MMA-co-MAL-Si) exhibiting characteristic red or green emissions of Eu or Tb ions. Especially the luminescent quantum efficiencies of europium hybrid systems are estimated and discussed in detail.

© 2008 Elsevier B.V. All rights reserved.

**Keywords:** Polymer hybrid material; Covalently bonded; Rare earth ion; Photoluminescence

## 1. Introduction

Encapsulation of rare earth complexes within stable inorganic hosts has been investigated thoroughly due to its combination of mutual advantages. Concentration on the lanthanide complexes has grown considerably since Lehn pointed out that such complexes could be used as light conversion molecular devices [1] namely the term “antenna effect” to describe the absorption, energy transfer, emission processes, thus solving the problem of very small absorption coefficients of the lanthanide ions. The design of efficient rare earth complexes has acquired the attention of many research groups, focusing on the diverse classes of ligands,  $\beta$ -diketones [2], heterobiaryl ligands [3], etc. Our research group is focusing on the lanthanide ions (Eu, Tb, Sm, Dy) complexes with aromatic carboxylic acid, bipyridyl or their derivatives [4–8]. But the main drawback of the com-

mon silica-doped materials seems difficult to solve the problem of quenching effect of emission centers because the high energy vibration by the surrounding hydroxyl groups and only weak interactions (such as hydrogen bonding, van der Waals force or weak static effect) functionalize between organic and inorganic parts [9]. Furthermore, inhomogeneous dispersion of two phases and leaching of the photoactive molecules frequently occur in this sort of hybrid materials for which the concentration of complexes is also largely impeded. In this way, another interesting idea in regard to the complexation of the lanthanides by ligands that are covalently bonded with hybrid networks has emerged. In past decades, the preparation methods have gradually turned into covalently bonded hybrids [10–18] in contrast to the traditional doping silica gels [19,20]. Some previous researches have concentrated on the modification of pyridine-dicarboxylic acid or their derivatives [21]. Zhang and coworkers focused on modification of heterocyclic ligands including 1,10-phenanthroline and di-pyridine [10,11] in order to construct molecular-based hybrids. Our research team presently did extensive work in the preparation of functional systems covalently connecting both

\* Corresponding author. Tel.: +86 21 65984663; fax: +86 21 65982287.  
E-mail address: [byan@tongji.edu.cn](mailto:byan@tongji.edu.cn) (B. Yan).

siliceous backbone and photoactive organic units [21–30]. In view of these researches, it can be recognized that the key procedure to construct molecular-based materials is to design “functional bridge molecule” by the grafting reaction which can behave double functions of both coordinating lanthanide ions and sol–gel processing to constitute covalent Si–O network [21–30]. However, several disadvantages still have made them excluded from practical uses, essentially because rare earth complexes and their silica hybrids lack the desired mechanical flexibility or they have difficulty in processing.

On the grounds of inheriting the merits of both the pure emission color of lanthanide ions and plastic properties of polymer material, luminescent polymer-based rare earth materials have come into being recently [31–38]. Wang et al. [36] have prepared Eu(III)-acrylate- $\beta$ -diketones monomers and methyl methacrylate (MMA) copolymers, indicating that Eu-complexes are uniformly bonded to the polymer chain. In this report, we initially prepared the copolymer of MMA and maleic anhydride (MAL) which was modified by 3-aminopropyltriethoxysilane (APES), then two kinds of highly efficient luminescent rare earth (RE) covalently bonded hybrid materials were in situ fabricated by two-step reactions simultaneously. The first one is rare earth ions coordinated to the carboxylic groups of MAL and the other triggers the hydrolysis/polycondensation process between triethoxysilyl and TEOS.

## 2. Experimental section

### 2.1. Chemicals and procedures

3-Aminopropyltriethoxysilane (APES) was purchased from Shanghai YaoHua chemical plant and purified by vacuum distillation. The collected fraction was 80 °C/0.27 kPa. MAL, analytic purity, provided from China Medicine Group Shanghai Chemical Reagent Corporation. MMA, 2,2-azo-bis-isobutyronitrile (AIBN) and tetrahydrofuran are domestic chemical products and purified using common methods. Tetraethoxysilane (TEOS) was used without further purification. A typical procedure for the preparation of co-polymers (MMA-co-MAL) was by radical polymerization of MMA (25 ml) and MAL (47 mmol) in 30 ml dehydrate tetrahydrofuran solution using 150 mg AIBN as initiator. Argon was introduced into the mixture for 1 h in order to expel the effect of oxygen. The flask was sealed and temperature retained at 65 °C for 36 h. The yield is 82% after purification applying methanol as precipitation agent. The content of MAL unit in co-polymer is 16 mol%, as determined by <sup>1</sup>H NMR spectroscopy. The number average molecular weight and molecular dispersity of co-polymers were  $2.4 \times 10^4$  and 2.58, respectively, as determined with gel-permeation chromatography (GPC) calibrated by polystyrene standards. The preparation of terbium containing hybrids was as follows: 1.0 g co-polymer was dissolved in 10 ml THF with stirring, 0.4 ml APES was added to the solution under argon and the stirring continues. One hour later, rare earth chloride TbCl<sub>3</sub>·6H<sub>2</sub>O (1.72 mmol, 0.64 g) and 0.341 g (0.682 g) 1,10-phenanthroline were introduced with stirring for 2 h. At last, TEOS and water (TEOS:H<sub>2</sub>O:TbCl<sub>3</sub>·6H<sub>2</sub>O = 5:18:1) were added to the above

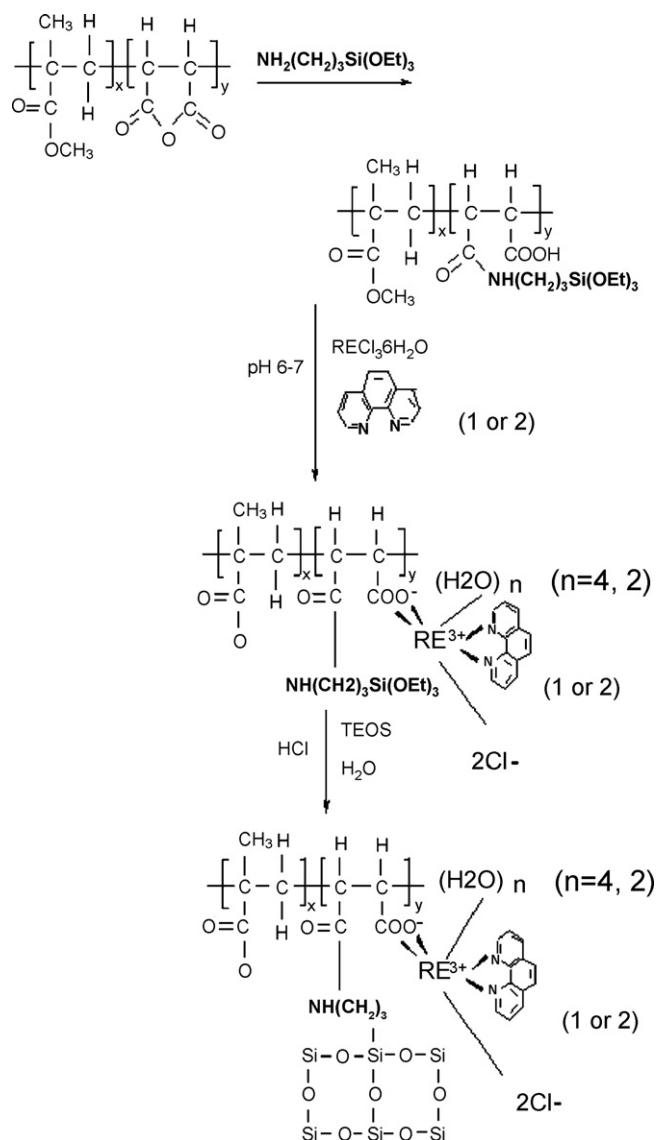


Fig. 1. Predicted structure of rare earth containing molecular-based hybrid material constructed by copolymers and TEOS.

solution with HCl readjusting pH of 1–2. The resulting solution was stirred for 2 h and transferred to another beaker, covered with a piece of parafilm. After gelling, some pinholes were made in the film and the mixture was left to dry at room temperature for 2 weeks and cured at 70 °C under vacuum for 24 h for the sake of getting rid of remaining alcohol and solvents (see Fig. 1). The corresponding Eu covalently bonded hybrids were prepared as the same procedure except for EuCl<sub>3</sub>·6H<sub>2</sub>O (1.72 mmol, 0.62 g) was used.

The concentration of Ln<sup>3+</sup> ions in covalent hybrids was measured under the traditional complexometric titration method. The final hybrid samples were dissolved in nitric acid, and then titrated with EDTA solution, using a buffer (pH 5.8) and xylenol-orange as indicator. Anal. Calcd. for [Ln(MMA-co-MAL-Si)(phen)(H<sub>2</sub>O)<sub>4</sub>]Cl<sub>2</sub>·5SiO<sub>2</sub> (Ln = Eu, Tb): C 38.00, H 5.16, N 2.59, Eu 9.38; found: C 37.76, H 4.91, N 2.39, Eu 9.58. Anal. Calcd. C 37.82, H 5.14, N 2.58, Tb 9.76; found: C 38.01, H 4.84, N 2.37, Tb 9.55. Anal. Calcd. for [Ln(MMA-co-MAL-

Si)(phen)<sub>2</sub>(H<sub>2</sub>O)<sub>2</sub>]Cl<sub>2</sub>·5SiO<sub>2</sub> (Ln = Eu, Tb): C 43.05, H 4.97, N 3.97, Eu 8.61; found: C 43.80, H 4.81, N 3.84, Eu 8.42. Anal. Calcd. C 42.88, H 4.95, N 3.95, Tb 8.97; found: C 43.06, H 4.74, N 3.77, Tb 9.14.

## 2.2. Measurements

All measurements were completed under room temperature. FT-IR spectra were measured within the 4000–400 cm<sup>-1</sup> region on an infrared spectrophotometer with the KBr pellet technique. Elemental analyses (C, H and N) were performed with an Elementar Carlo EL elemental analyzer. Differential scanning calorimetry (DSC) was performed on a TA DSCQWo, and the heating rate and nitrogen flow rate were 10 °C/min and 20 ml/min, respectively. Low temperature phosphorescence spectrum ( $5 \times 10^{-5}$  mol l<sup>-1</sup> acetone solution) was determined by PerkinElmer LS-55 spectrophotometer under 77 K. Fluorescent excitation and emission spectrums were obtained on a PerkinElmer LS-55 spectrophotometer: excitation slit width = 10 nm, emission slit width = 5 nm. All the emission and excitation spectra were corrected and the intensities were determined with integrated area. Luminescent lifetimes for hybrid materials were obtained with an Edinburgh Instruments FLS 920 phosphorimeter using a 450-W xenon lamp as excitation source (pulse width, 3 μs). The microstructures were checked by scanning electronic microscope (SEM, Philips XL-30). The atomic force microscopy (AFM) image was obtained in the tapping mode on a NanoScope IIIA MultiMode AFM with a hot stage, at temperatures in the range of 20–50 °C: the powder sample was treated by dispersing in water by super-sonication, after which a droplet of water containing sample was put onto a hydrophilic silicon wafer.

## 3. Results and discussion

### 3.1. Characterization of the hybrid materials

Fig. 1 shows the scheme of the hybrid materials. The copolymer possesses the functional MAL unit which can be modified with APES to form the amide group and carboxylate group. As the previous research, it can be found that the derivative of MAL generally only provides one coordination group of carboxylate for its coordination ability is stronger than that of amide or ester groups [39,40]. Besides, the limited space hinders the neighbor group coordinates simultaneously [39,40]. The modified copolymer derivative behaves as a functional bridge to rare earth ions through the carboxylates and forms Si–O network with TEOS after a cohydrolysis and copolycondensation process. First, rare earth chloride was used as precursor salts for Cl<sup>-</sup> has weak coordination ability to rare earth ions, which makes it easy to understand the coordination environment surrounding the central RE<sup>3+</sup>. Phen behaves as the functional ligands for its coordination behavior is simple chelation to RE<sup>3+</sup> with two nitrogen atoms. So there exists the empty coordination spot to accept the oxygen atoms of coordination water molecules. All the coordination environment of RE<sup>3+</sup> can be verified further by the following characterization.

Fig. 2 shows the selected FT-IR spectra of (A) co-polymers (MMA-co-MAL) and (B) covalently bonded Tb hybrids. In the spectrum of A, three distinctive peaks were observed to locate at 1855, 1786 and 1733 cm<sup>-1</sup>. The band at 1733 cm<sup>-1</sup> is ascribed to the stretching vibration of the C=O groups of the MMA units, the other two peaks are attributed to the vibration of MAL. As for the spectrum B, the absorption at 1733 cm<sup>-1</sup> was still there indicating the MMA units existed in the result-

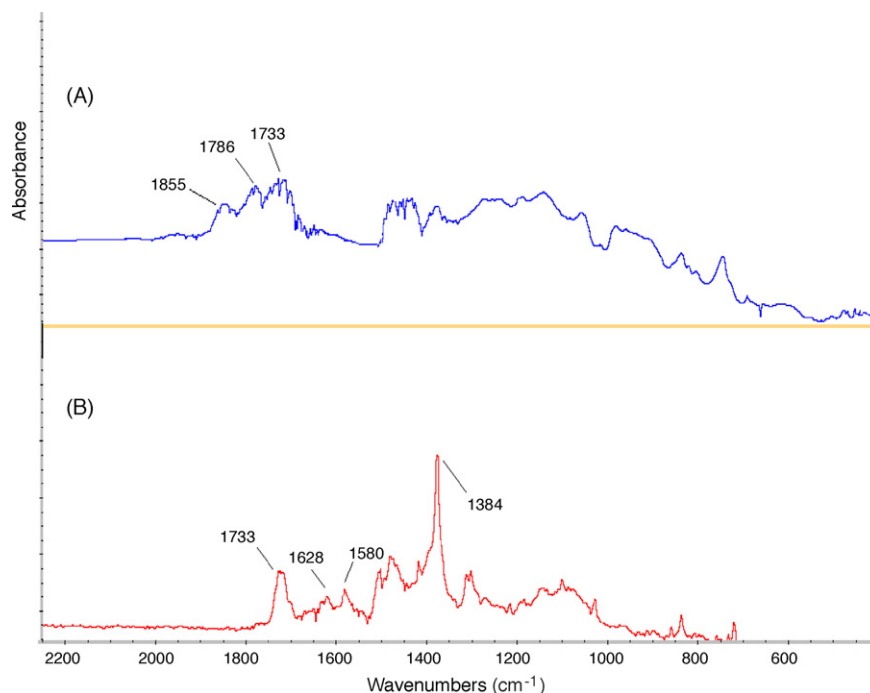


Fig. 2. FT-IR spectra of (A) co-polymers (MMA-co-MAL) and (B) Tb-containing hybrids.

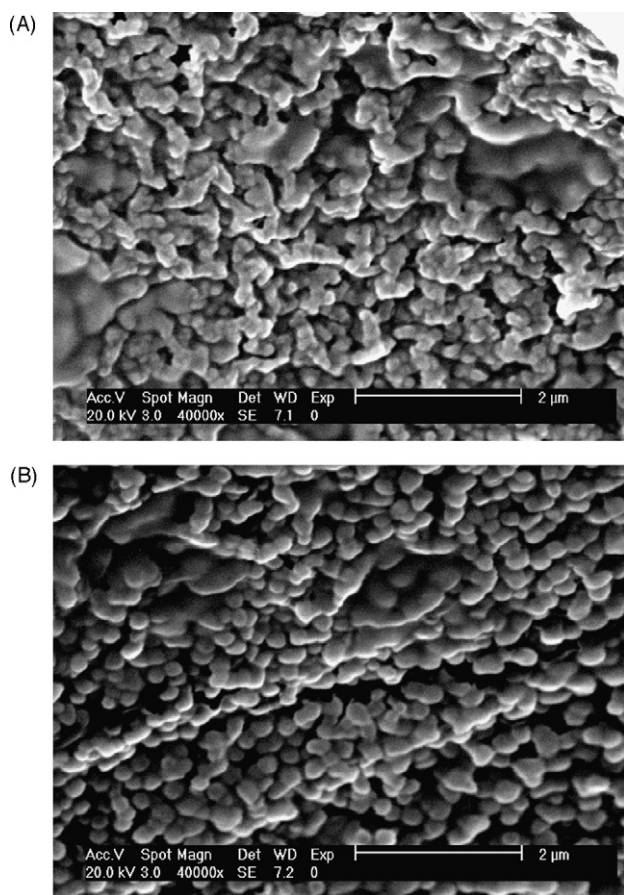


Fig. 3. SEM for (A) phen-Tb-MMA-co-MAL-Si and (B) 2phen-Tb/MMA-co-MAL-Si.

ing hybrid materials. But two new peaks emerged, at 1628 and 1580  $\text{cm}^{-1}$ . In terms of Socrates' discussion [41], the two bands are due to amide I and amide II, exhibiting the successful grafting reaction between MAL and amino group of APES. Besides, so far as the ternary covalently bonded systems are concerned, the occurrence of complexation between  $\text{Tb}^{3+}$  and MMA-co-MAL evidenced by a new narrow band located at 1383–1387  $\text{cm}^{-1}$  and 1596–1604  $\text{cm}^{-1}$  appeared to prove that terbium ions may coordinate to two oxygen atoms of the free carboxylic groups. The twisting bending vibrations at 896, 761 and 857, 743  $\text{cm}^{-1}$  which correspond to absorption of hydrogen atoms belong to heterocycle of phen have shifted to lower frequency of 854, 727  $\text{cm}^{-1}$ , and the facts firmly prove phen can coordinate to lanthanide ions effectively.

Fig. 3 compared the micromorphology of the two kinds of covalently bonded europium hybrid materials, which verifies that a homogeneous, molecular-based system was obtained because of strong covalent bonds bridging between the inorganic and organic phase which belongs to a complicated huge molecule in nature, and that they are composed quite uniformly so that the two phases can exhibit their distinct properties together, which overcome the disadvantages of that the hybrid systems with doped rare earth complexes generally experience phase separation phenomena [22,26]. Ulteriorly, compared

with the two SEM pictures, there exists a little distinction between these covalently bonded hybrid materials and the organic copolymer chain unit have strong influence on the microstructure and morphology of the hybrid systems. The introduction of copolymer chain fulfils the template to induce the formation of regular microstructure. Especially the 2phen-Tb-MMA-co-MAL-Si hybrids present the ordered particle with 100–200 nm dimension, which suggests that the terminal ligand of phen also affects the micromorphology of hybrid system. Fig. 4 shows the AFM photographs of the surface of hybrid materials Eu-containing hybrids. On the basis of images of the atomic force microscopy, it is quite attractive that the covalent composites exhibit some relatively regular column shapes (diameter range with around 200 nm dimension) within rough top surfaces that maybe caused by mutual influences originated from polymeric soft chains and silica coupling agent simultaneously. Besides, no corresponding phase separation phenomenon was observed.

### 3.2. Luminescent properties

As shown in Fig. 5, the phosphorescence spectra of phen-Gd-MMA-co-MAL-Si at 77 K wears the feature of phen, substantiating that the heterocyclic ligand will become main energy donor and have the possibility to sensitize  $\text{Eu}^{3+}$  and  $\text{Tb}^{3+}$  ions. According to the energy transfer and intramolecular energy mechanism [4,5], intramolecular energy transfer efficiency depends chiefly on two energy transfer processes: the first one leads from the triplet level of ligands to the emissive energy level of the  $\text{Eu}^{3+}$  and  $\text{Tb}^{3+}$  ion by Dexter's resonant exchange interaction [40]; the second one is just an inverse energy transfer by a thermal deactivation mechanism [41]. Established on this theory, the conclusion can be drawn that energy differences is of opposite influence on the two energy transfer processes and an optimal value can be assumed to exist. So phen (453 nm, 22,075  $\text{cm}^{-1}$ ) has a suitable energy match to  $\text{Eu}^{3+}$  and  $\text{Tb}^{3+}$  and can achieve the effective luminescence of hybrid systems [4,5].

The selected excitation and emission spectra of the resulting 2phen-Tb(Eu)MMA-co-MAL-Si are shown in Figs. 6 and 7. The excitation spectra (Fig. 6) was obtained by monitoring the emission of  $\text{Tb}^{3+}$  at 545 nm. The maximum absorption of the hybrid materials occurred within the range of 280–350 nm and dominated by peak centered at 342 nm which may be resulted from conjugating  $\pi-\pi^*$  transition of the 1,10-phenanthroline. As a result, the emission lines of the hybrid material were obtained from the  $^5\text{D}_4 \rightarrow ^7\text{F}_j$  ( $J=6, 5, 4, 3$ ) transitions at 490, 544, 587 and 622 nm for terbium ions (Fig. 6) under the excitation wavelength at 342 nm. Among these emission peaks, the most striking green luminescence ( $^5\text{D}_4 \rightarrow ^7\text{F}_5$ ) was observed in their emission spectra which indicated that the effective energy transfer took place between the 1,10-phenanthroline and the chelated Tb ions. Fig. 7 gives the excitation and emission spectra of Eu covalent hybrids, the absorption proves results similar to Fig. 6, revealing that 1,10-phenanthroline plays a key role as a energy donor. Five emission peaks located at 536, 590, 614, 650 and 700 nm were assigned to the  $^5\text{D}_1 \rightarrow ^7\text{F}_1$ ,  $^5\text{D}_0 \rightarrow ^7\text{F}_j$



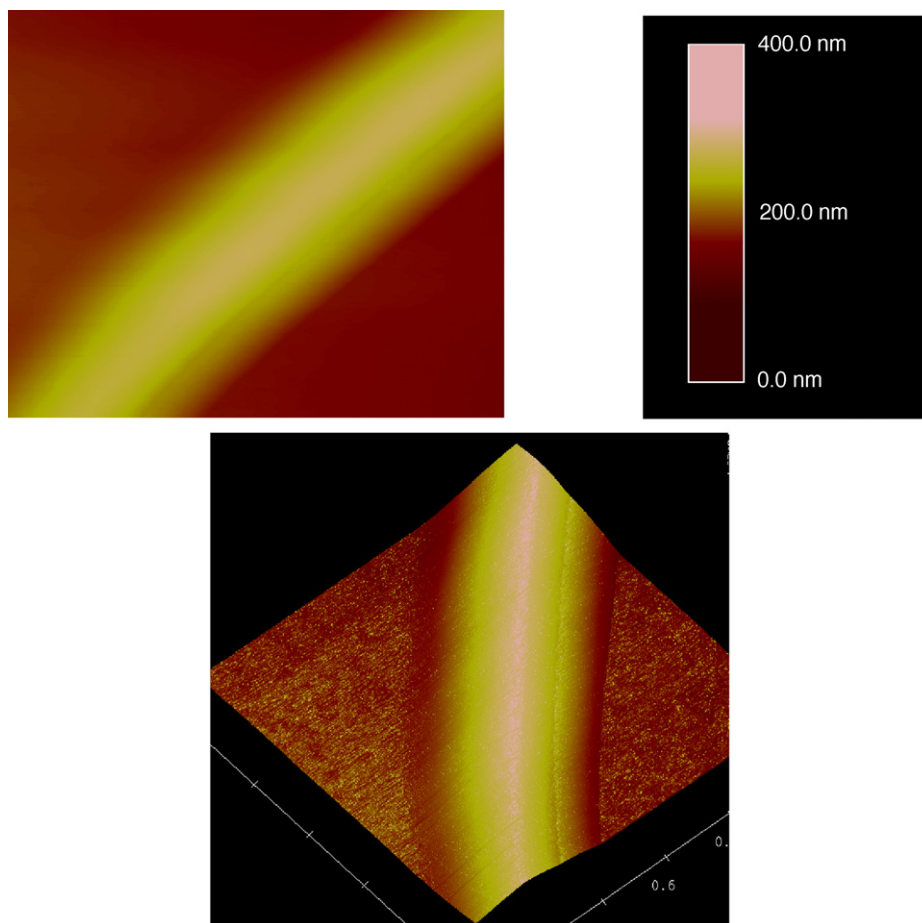


Fig. 4. AFM photographs of the surface of 2phen-Eu-MMA-co-MAL-Si.

( $J = 1, 2, 3, 4$ ) transitions, respectively. Among these bands, the emission at 614 nm due to the  ${}^5D_0 \rightarrow {}^7F_2$  electro-dipolar transition is the strongest, indicating low symmetry environment around the Eu(III) ion in the hybrids. Generally speaking, the forbidden  ${}^5D_0 \rightarrow {}^7F_2$  electro-dipole transition is rather sensitive to the coordinative environment of Eu ions, it is evident that the polymer-inorganic-based asymmetric micro-chemical environment leads to the polarization of the Eu(III) ion in regard to the influence of electric field of the coordinating ligands, which enhances the probability for the  ${}^5D_0 \rightarrow {}^7F_2$  transition.

The typical decay curve of the Eu and Tb hybrid materials were measured and they can be described as a single exponential ( $\ln(S(t)/S_0) = -k_1t = -t/\tau$ ), indicating that all  $\text{Eu}^{3+}$  and  $\text{Tb}^{3+}$  ions occupy the same average coordination environment. The resulting lifetime data of Eu and hybrids were given in Table 1. It was found that the lifetimes of 2phen-Eu(Tb)-MMA-co-MAL-Si are longer than that of phen-Eu(Tb)-MMA-co-MAL-Si, suggesting that the introduction of phen can enhance the luminescence stability of the whole hybrid systems. Further, we selectively determined the emission quantum efficiencies of the  ${}^5D_0$  excited state of europium ion for  $\text{Eu}^{3+}$  hybrids on the basis of the emission spectra and lifetimes of the  ${}^5D_0$  emitting level, the detailed luminescent data were shown in Table 1. The quantum efficiency of the luminescence step,  $\eta$  expresses how well the

radiative processes (characterized by rate constant  $A_r$ ) compete with non-radiative processes (overall rate constant  $A_{nr}$ ) [42–50].

$$\eta = \frac{A_r}{A_r + A_{nr}} \quad (1)$$

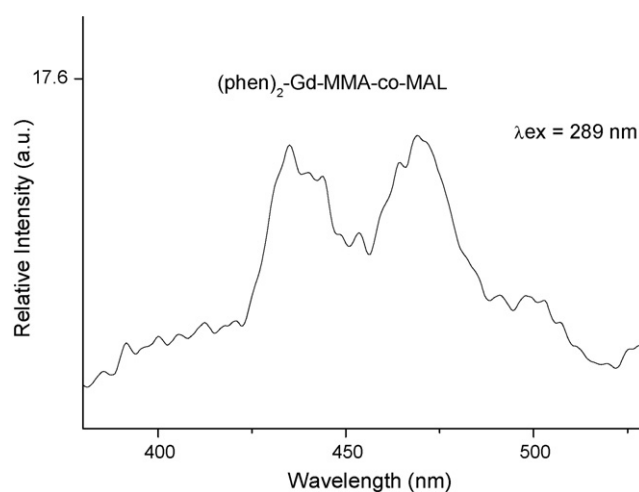


Fig. 5. Phosphorescence spectra of 2phen-Gd-MMA-co-MAL ternary complex ( $5 \times 10^{-5} \text{ mol l}^{-1}$  acetone solution).

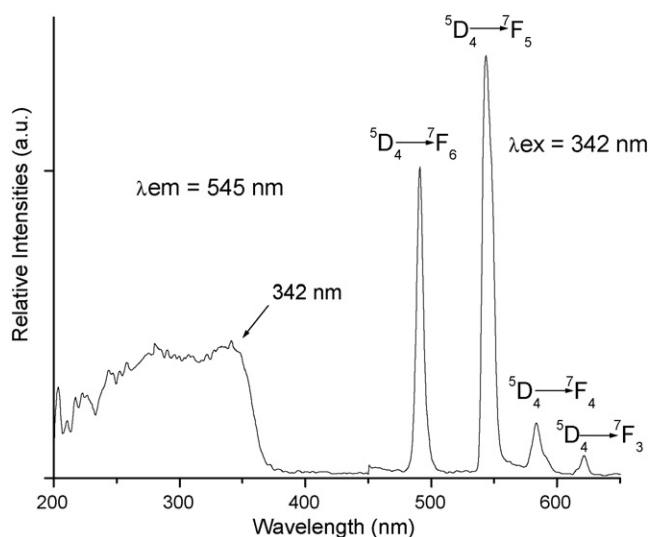


Fig. 6. Selected excitation and emission spectra of the covalently bonded Tb hybrid material 2phen-Tb-MMA-co-MAL-Si.

Non-radiative processes influence the experimental luminescence lifetime by the equation [42–50]:

$$\tau_{\text{exp}} = (A_r + A_{\text{nr}})^{-1} \quad (2)$$

So quantum efficiency can be calculated from radiative transition rate constant and experimental luminescence lifetime from the following equation [42–50]:

$$\eta = A_r \tau_{\text{exp}} \quad (3)$$

where  $A_r$  can be obtained by summing over the radiative rates  $A_{0J}$  for each  ${}^5D_0 \rightarrow {}^7F_J$  transitions of  $\text{Eu}^{3+}$  [42–50].

$$A_r = \sum A_{0J} = A_{00} + A_{01} + A_{02} + A_{03} + A_{04} \quad (4)$$

The branching ratio for the  ${}^5D_0 \rightarrow {}^7F_{5,6}$  transitions can be neglected as they both are not detected experimentally, whose influence can be ignored in the depopulation of the  ${}^5D_0$  excited

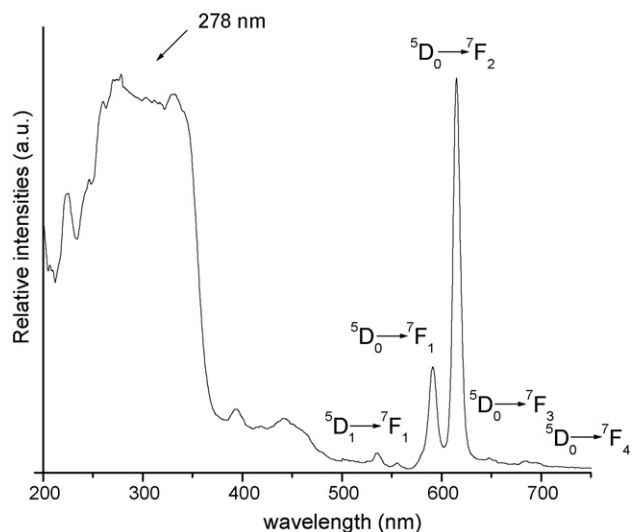


Fig. 7. Selected excitation and emission spectra of the covalently bonded Eu hybrid material 2phen-Eu-MMA-co-MAL-Si.

Table 1

The luminescence efficiencies and lifetimes of the solid covalent hybrids

Systems	Phen-Eu-MMA-co-MAL	2Phen-Eu/MMA-co-MAL-Si
$\nu_{00}$ ( $\text{cm}^{-1}$ ) <sup>a</sup>	17167	17153
$\nu_{01}$ ( $\text{cm}^{-1}$ ) <sup>a</sup>	16906	16906
$\nu_{02}$ ( $\text{cm}^{-1}$ ) <sup>a</sup>	16248	16234
$\nu_{03}$ ( $\text{cm}^{-1}$ ) <sup>a</sup>	15408	15408
$\nu_{04}$ ( $\text{cm}^{-1}$ ) <sup>a</sup>	14327	14347
$\tau$ (ms) <sup>b</sup>	0.25	0.41
$A_{\text{rad}}$ ( $\text{s}^{-1}$ )	314	320
$\tau_{\text{exp}}^{-1}$ ( $\text{s}^{-1}$ )	4000	2439
$A_{\text{nrad}}$ ( $\text{s}^{-1}$ )	3686	2019
$\eta$ (%)	7.85	13.12
$n_w$	3.87	2.12
Systems	Phen-Tb-MMA-co-MAL-Si	2Phen-Tb/MMA-co-MAL-Si
$\tau$ (ms) <sup>c</sup>	0.49	0.77
Emission bands	489, 544.5, 58, 622	489, 544.5, 588, 621.5

<sup>a</sup> The energies of the  ${}^5D_0 \rightarrow {}^7F_J$  transitions ( $\nu_{0J}$ ).

<sup>b</sup> For  ${}^5D_0 \rightarrow {}^7F_2$  transition of  $\text{Eu}^{3+}$ .

<sup>c</sup> For  ${}^5D_4 \rightarrow {}^7F_5$  transition of  $\text{Tb}^{3+}$ .

state [44–46]. Since  ${}^5D_0 \rightarrow {}^7F_1$  belongs to the isolated magnetic dipole transition, it is practically independent of the chemical environments around the  $\text{Eu}^{3+}$  ion, and thus can be considered as an internal reference for the whole spectrum, the experimental coefficients of spontaneous emission,  $A_{0J}$  can be calculated according to the relation [47]:

$$A_{0J} = A_{01} \left( \frac{I_{0J}}{I_{01}} \right) \left( \frac{\nu_{01}}{\nu_{0J}} \right) \quad (5)$$

Here  $A_{0J}$  is the experimental coefficient of spontaneous emission, among  $A_{01}$  is the Einstein's coefficient of spontaneous emission between the  ${}^5D_0$  and  ${}^7F_1$  energy levels. In vacuum,  $A_{01}$  as a value of  $14.65 \text{ s}^{-1}$ , when an average index of refraction  $n$  equal to 1.506 was considered, the value of  $A_{01}$  can be determined to be  $50 \text{ s}^{-1}$  approximately ( $A_{01} = n^3 A_{01}(\text{vacuum})$ ) [43,48].  $I$  is the emission intensity and can be taken as the integrated intensity of the  ${}^5D_0 \rightarrow {}^7F_J$  emission bands [49,50].  $\nu_{0J}$  refers to the energy barrier and can be determined from the emission bands of  $\text{Eu}^{3+}$ 's  ${}^5D_0 \rightarrow {}^7F_J$  emission transitions. Here the emission intensity,  $I$ , taken as integrated intensity  $S$  of the  ${}^5D_0 \rightarrow {}^7F_{0-4}$  emission curves, can be defined as below

$$I_{i-j} = \hbar \omega_{i-j} A_{i-j} N_i \approx S_{i-j} \quad (6)$$

where  $i$  and  $j$  are the initial ( ${}^5D_0$ ) and final levels ( ${}^7F_{0-4}$ ), respectively,  $\omega_{i-j}$  is the transition energy,  $A_{i-j}$  is the Einstein's coefficient of spontaneous emission, and  $N_i$  is the population of the  ${}^5D_0$  emitting level. On the basis of the above discussion, the quantum efficiency of the three kinds of europium polymeric hybrid materials can be determined and shows the similar rule to their lifetimes. 2Phen-Eu-MMA-co-MAL-Si presents the higher quantum efficiency than phen-Eu-MMA-co-MAL-Si for the more molar ratio of phen, which can provide the more energy donor and avoid the non-radiative energy loss of coordinated water molecules.

In order to study the coordination environment surrounding lanthanide ions especially the influence caused by vibrations

of water molecules, according to Horrocks' previous research [51,52] it is therefore expected that probable number of coordinated water molecules ( $n_w$ ) can be calculated as following equations:

$$n_w = 1.05(A_{\text{exp}} - A_{\text{rad}}) \quad (7)$$

$$A_{\text{exp}} = \frac{1}{\tau_{\text{exp}}} = A_{\text{rad}} + A_{\text{nr}} \quad (8)$$

in which  $k_r$  and  $k_{nr}$  are radiative and non-radiative probabilities, respectively.  $\tau_{\text{exp}}$  is decay time of Eu-containing covalent hybrids.  $k_r$  can be described as the ratio of relative intensities of  ${}^5D_0 \rightarrow {}^7F_J$  ( $J=6, 5, 4, 3$ ) transitions. The values of  $A_{\text{rad}}$ ,  $A_{\text{nr}}$  and  $n_w$  were calculated through the above three equations and reported in Table 1. Based on the results, the coordination number of water molecules (Eu-containing hybrid materials) can be estimated to be four and two for phen-Eu-MMA-co-MAL-Si and 2phen-Eu-MMA-co-MAL-Si, respectively. The coordination water molecules produce the severe vibration of hydroxyl group, resulting in the large non-radiative transition and decreasing the luminescent efficiency.

#### 4. Conclusions

A novel class of RE-containing hybrid materials was prepared in the presence of APES. The co-polymer MMA-co-MAL was introduced into the inorganic matrices due to strong covalent bonds through the aminolytic reactions between the MAL components and the amino group on APES. Subsequently, the coordination reactions among rare earth ions, carboxylic groups of MAL and 1,10-phenanthroline happened at the same moment with the hydrolytic polycondensation process of the triethoxysilyl group bearing polymer and TEOS. FTIP and DSC analysis proved the existence of amide groups in the hybrid materials. In addition, the introduction of molar ratio of phen enhances the luminescent lifetimes and quantum efficiency of covalently bonded hybrid systems.

#### Acknowledgement

This work was supported by the National Natural Science Foundation of China (20671072).

#### References

- [1] J.M. Lehn, *Angew. Chem. Int. Ed. Engl.* 29 (1990) 1304–1319.
- [2] G.F. de Sa, O.L. Malta, C. Mello Donega, A.M. Simas, R.L. Longo, P.A. Santa-Cruz, E.F. da Silva Jr., *Coord. Chem. Rev.* 196 (2000) 165–195.
- [3] H. Takalo, V.M. Mikkala, L. Merio, J.C. Rodriguez-Ubis, R. Sedano, O. Juanes, E. Brunet, *Helv. Chim. Acta* 80 (1997) 372–387.
- [4] Y.S. Song, B. Yan, Z.X. Chen, *J. Solid State Chem.* 177 (2004) 3805–3814.
- [5] B. Yan, B. Zhou, *J. Photochem. Photobiol. A: Chem.* 171 (2005) 181–186.
- [6] B. Yan, Y.Y. Bai, X.X. Chen, *J. Mol. Struct.* 741 (2005) 141–148.
- [7] S.Y. Song, B. Yan, *Inorg. Chim. Acta* 358 (2005) 191–195.
- [8] S.Y. Song, B. Yan, Z.X. Chen, *Polyhedron* 26 (2007) 4591–4601.
- [9] C. Sanchez, F. Ribot, *New J. Chem.* 18 (1994) 1007–1047.
- [10] H.R. Li, J. Lin, H.J. Zhang, H.C. Li, L.S. Fu, Q.G. Meng, *Chem. Commun.* (2001) 1212–1213.
- [11] H.R. Li, J. Lin, H.J. Zhang, L.S. Fu, Q.G. Meng, S.B. Wang, *Chem. Mater.* 14 (2002) 3651–3655.
- [12] K. Binnemans, P. Lenaerts, K. Driesen, C. Gorller-Walrand, *J. Mater. Chem.* 14 (2004) 191–196.
- [13] D.W. Dong, S.C. Jiang, Y.F. Men, X.L. Ji, B.Z. Jiang, *Adv. Mater.* 12 (2000) 646–649.
- [14] A.C. Fraville, R. Mahiou, D. Zambon, J.C. Cousseins, *Solid State Sci.* 3 (2001) 211–222.
- [15] L.D. Carlos, R.A.S. Ferreira, J.P. Rainho, V. de Zea Bermudez, *Adv. Funct. Mater.* 12 (2002) 819–823.
- [16] L.D. Carlos, R.A.S. Ferreira, R.N. Pereira, M. Assuncao, V. de Zea Bermudez, *J. Phys. Chem. B* 108 (2004) 14924–14932.
- [17] M.C. Goncalves, V.Z. Bermudez, R.A.S. Ferreira, L.D. Carlos, D.J. Rocha, *Chem. Mater.* 16 (2004) 2530–2543.
- [18] S.S. Nobre, P.P. Lima, L. Mafra, R.A.S. Ferreira, R.O. Freire, L.S. Fu, U. Pischel, V.Z. Bermudez, O.L. Malta, L.D. Carlos, *J. Phys. Chem. C* 111 (2007) 3275–3284.
- [19] L.R. Matthews, E.T. Knobbe, *Chem. Mater.* 5 (1993) 1697–1703.
- [20] P.A. Tanner, B. Yan, H.J. Zhang, *J. Mater. Sci.* 35 (2000) 4325–4329.
- [21] Q.M. Wang, B. Yan, *J. Mater. Chem.* 14 (2004) 2450–2455.
- [22] Q.M. Wang, B. Yan, *Cryst. Growth Des.* 5 (2005) 497–503.
- [23] Q.M. Wang, B. Yan, *J. Photochem. Photobiol. A: Chem.* 78 (2006) 70–75.
- [24] Q.M. Wang, B. Yan, *J. Organomet. Chem.* 691 (2006) 540–545.
- [25] B. Yan, D.J. Ma, *J. Solid State Chem.* 179 (2006) 2059–2066.
- [26] Q.M. Wang, B. Yan, *J. Mater. Res.* 20 (2005) 592–598.
- [27] Q.M. Wang, B. Yan, *J. Photochem. Photobiol. A: Chem.* 178 (2006) 159–165.
- [28] B. Yan, F.F. Wang, *J. Organomet. Chem.* 692 (2007) 2395–2402.
- [29] B. Yan, X.F. Xiao, *Photochem. Photobiol.* 83 (2007) 971–977.
- [30] Q.M. Wang, B. Yan, *J. Organomet. Chem.* 691 (2006) 3567–3573.
- [31] Y.J. Okamoto, *Macromol. Sci. Chem. A* 24 (1987) 455–460.
- [32] R. Iwamura, N. Higashiyama, K. Takemura, K.S. Tsutsumi, K. Kimura, G. Adachi, *Chem. Lett.* (1994) 1131–1134.
- [33] H.Y. Chen, R.D. Archer, *Macromolecules* 29 (1996) 1957–1964.
- [34] H.H. Qin, J.H. Dong, K.Y. Qiu, Y. Wei, *J. Appl. Polym. Sci.* 78 (2000) 1763–1768.
- [35] V. Bekiari, G. Pistolis, P. Lianos, *Chem. Mater.* 11 (1999) 3189–3195.
- [36] L.H. Wang, W. Wang, W.G. Zhang, E.T. Kang, W. Huang, *Chem. Mater.* 12 (2000) 2212–2218.
- [37] Q.M. Wang, B. Yan, *J. Photochem. Photobiol. A: Chem.* 177 (2006) 1–5.
- [38] Y.H. Luo, Q. Yan, S. Wu, W.X. Wu, Q.J. Zhang, *J. Photochem. Photobiol. A: Chem.* 191 (2007) 91–96.
- [39] A.C. Franville, D. Zambon, R. Mahiou, *Chem. Mater.* 12 (2000) 428–435.
- [40] D.L. Dexter, *J. Chem. Phys.* 21 (1953) 836–841.
- [41] T.D. Brown, T.M. Shepherd, *J. Chem. Soc., Dalton Trans.* 3 (1973) 336–344.
- [42] M.H.V. Werts, R.T.F. Jukes, J.M. Verhoeven, *Phys. Chem. Chem. Phys.* 4 (2002) 1542–1548.
- [43] C.Y. Peng, H.J. Zhang, J.B. Yu, Q.G. Meng, L.S. Fu, H.R. Li, L.N. Sun, X.M. Guo, *J. Phys. Chem. B* 109 (2005) 15278–15287.
- [44] L.D. Carlos, Y. Messaddeq, H.F. Brito, R.A.S. Ferreira, V.D. Bermudez, S.J.L. Ribeiro, *Adv. Mater.* 12 (2000) 594–598.
- [45] R.A.S. Ferreira, L.D. Carlos, R.R.G.E. Silva, S.J.L. Ribeiro, V.D. Bermudez, *Chem. Mater.* 13 (2001) 2991–2998.
- [46] P.C.R. Soares-Santos, H.I.S. Nogueira, V. Felix, M.G.B. Drew, R.A.S. Ferreira, L.D. Carlos, T. Trindade, *Chem. Mater.* 15 (2003) 100–108.
- [47] E.E.S. Teotonio, J.G.P. Espynola, H.F. Brito, O.L. Malta, S.F. Oliveria, D.L.A. de Faria, C.M.S. Izumi, *Polyhedron* 21 (2002) 1837–1844.
- [48] S.J.L. Ribeiro, K. Dahmouche, C.A. Ribeiro, C.V. Santilli, S.H.J. Pulcinelli, *J. Sol-Gel Sci. Technol.* 13 (1998) 427–432.
- [49] O.L. Malta, M.A. Couto dos Santos, L.C. Thompson, N.K. Ito, *J. Lumin.* 69 (1996) 77–84.
- [50] O.L. Malta, H.F. Brito, J.F.S. Menezes, R.R.G.E. Silva, S. Alves, F.S. Farias, A.V.M. de Andrade, *J. Lumin.* 75 (1997) 255–268.
- [51] W.D. Horrocks, D.R. Sudnick, *J. Am. Chem. Soc.* 101 (1979) 334–340.
- [52] W.D. Horrocks, D.R. Sudnick, *Acc. Chem. Res.* 14 (1981) 384–392.